



# Absolute line intensities in methyl bromide: The 7- $\mu\text{m}$ region

F. Kwabia Tchana<sup>a,\*,1</sup>, D. Jacquemart<sup>a</sup>, N. Lacome<sup>a</sup>, I. Kleiner<sup>b</sup>, J. Orphal<sup>b</sup>

<sup>a</sup> Université Pierre et Marie Curie-Paris 6; CNRS; Laboratoire de Dynamique, Interactions et Réactivité, UMR 7075, Case Courrier 49, 4 Place Jussieu, 75252 Paris Cedex 05, France

<sup>b</sup> Laboratoire Inter-Universitaire des Systèmes Atmosphériques, UMR 7583 CNRS, Université Paris 12 et Paris 7, 61 avenue du Général de Gaulle, 94010 Créteil Cedex, France

Received 7 October 2005; in revised form 24 October 2005

## Abstract

This work deals, for the first time, with the modeling of absolute line intensities in the fundamental  $\nu_2$  and  $\nu_5$  bands of  $\text{CH}_3^{79}\text{Br}$  and  $\text{CH}_3^{81}\text{Br}$  at 7  $\mu\text{m}$ . For that, four unapodized absorption spectra of  $\text{CH}_3\text{Br}$  (natural abundance, 99% purity,  $P \times L = 0.082 - 0.165 \text{ atm} \times \text{cm}$ , room temperature) were measured in the range 1260–1560  $\text{cm}^{-1}$ , at a resolution of 0.002  $\text{cm}^{-1}$  using a Fourier transform spectrometer Bruker IFS 120 HR. For both isotopomers, 313 line intensities were analyzed within the dyad system required to account properly for the strong Coriolis coupling between  $\nu_2$  and  $\nu_5$ . The intensity fit of experimental data led to the determination of the dipole moment derivatives  $d_2 = \partial\mu/\partial q_2$  and  $d_5 = \partial\mu/\partial q_5$  relative to the  $\nu_2$  and  $\nu_5$  bands, as well as the first-order Herman–Wallis correction in  $K$  to  $d_5$ . The observed line intensities are fitted to 3.0% (3.3%) for  $\nu_2$  at 1309.9  $\text{cm}^{-1}$  and 2.6% (3.0%) for  $\nu_5$  at 1442.9  $\text{cm}^{-1}$ , respectively for  $\text{CH}_3^{79}\text{Br}$  and  $\text{CH}_3^{81}\text{Br}$ . The values derived for the vibrational band strengths of  $\nu_2$  and  $\nu_5$  are 55.7(0.6) and 39.2(0.3)  $\text{cm}^{-2} \text{atm}^{-1}$  at 296 K, respectively. The corresponding assignments and line positions of the dyad from previous work [F. Kwabia Tchana, I. Kleiner, J. Orphal, N. Lacome, O. Bouba, J. Mol. Spectrosc. 228 (2004) 441] are combined with the present intensity study to provide an improved  $\text{CH}_3\text{Br}$  database for atmospheric applications.

© 2005 Elsevier Inc. All rights reserved.

**Keywords:** Methyl bromide; Infrared spectra; Dyad; Line intensities; Dipole moment

## 1. Introduction

Methyl bromide ( $\text{CH}_3\text{Br}$ ) is an atmospheric trace gas of interest because of its contribution to stratospheric ozone depletion. Methyl bromide has both natural and anthropogenic origins. Its known sources include natural production from oceans [1] and biomass burning [2]. Methyl bromide is also industrially produced for use as an agricultural fumigant. With a tropospheric mixing ratio of 9–11 pptv in the Northern Hemisphere (with an increase of about 0.15 pptv per year) and about 8 pptv in the Southern Hemi-

sphere, it is believed to be the single largest contributor of stratospheric bromide [3]. However, until present, no attempts have been made to determine atmospheric concentrations of  $\text{CH}_3\text{Br}$  using infrared spectroscopy. For this, accurate modeling of the infrared spectrum of  $\text{CH}_3\text{Br}$ , including line intensities, is indispensable.

There have been various investigations in the past on the infrared and microwave spectra of methyl bromide. An extensive review of the spectroscopy of this molecule was given by Graner [4]. The most recent infrared work on this molecule including line intensities was published in 2002 by Brunetaud et al. [5]. In that work, high-resolution spectra of the  $\nu_6$  band of  $\text{CH}_3\text{Br}$  between 820 and 1120  $\text{cm}^{-1}$  were recorded and line positions and intensities were predicted for atmospheric remote-sensing applications.

Although the line positions in the 7- $\mu\text{m}$  region (containing the two interacting fundamentals  $\nu_2$  and  $\nu_5$ ) have been

\* Corresponding author. Fax: +33 1 49 40 32 00.

E-mail address: fkwabia@yahoo.fr (F.K. Tchana).

<sup>1</sup> Present address: Laboratoire de Physique des Lasers, UMR 7538 CNRS, Université Paris 13, 99 Avenue Jean Baptiste Clément, 93430 Villetaneuse, France.

Table 1  
Experimental conditions used to record the FTIR spectra of CH<sub>3</sub>Br<sup>a</sup>

Spectrum No.	Path (cm)	Pressure <sup>b</sup> (mbar)	Temperature (K)	Resolution (cm <sup>-1</sup> )
Bruker IFS 120 HR at LADIR, Paris, Bandpass: 1150–1550 cm <sup>-1</sup>				
1.	415 (1)	0.1991 (8)	297 (1)	0.002
2.	415 (1)	0.2778 (11)	296 (1)	0.002
3.	415 (1)	0.3415 (14)	298 (1)	0.002
4.	415 (1)	0.4028 (16)	296 (1)	0.002
5. <sup>c</sup>	27.0 (0.1)	4.693 (5)	296 (1)	0.004

Note. The resolution is equal to 0.9/(maximum optical path difference) and 1 atm = 1013 mbar.

<sup>a</sup> The numbers in parentheses represent the absolute uncertainty in the units of the last digit quoted.

<sup>b</sup> The absolute uncertainty is estimated to be 0.4% of the measured pressure.

<sup>c</sup> Recorded using the Bruker IFS 120 HR located at LPPM, Orsay (see [6] for more details).

reinvestigated recently at high spectral resolution [6], little is known about the line intensities in this region. The integrated band intensities of these two overlapping bands were measured in the past by different groups [7–10], using band separation techniques applied to low-resolution spectra. However, no line by line study of absolute intensities at 7 μm of CH<sub>3</sub>Br is presently available. At the present time, no spectroscopic information (including line positions, intensities, and linewidths) on CH<sub>3</sub>Br is available from either the HITRAN [11] or the GEISA [12] databases.

The purpose of the present study was to measure the absolute infrared intensities for the two fundamentals  $\nu_2$  and  $\nu_5$  of CH<sub>3</sub><sup>79</sup>Br and CH<sub>3</sub><sup>81</sup>Br, and to provide a CH<sub>3</sub>Br compilation at 7 μm for databases. The intensity parameters were derived by analyzing a set of individual line intensities accurately measured using a Fourier transform spectrometer Bruker IFS 120 HR. Modeling of the intensities was achieved within a two-interacting-band system, i.e.,  $\nu_2$  and  $\nu_5$ , such a model being required to account properly for the strong Coriolis coupling between  $\nu_2$  and  $\nu_5$ . The formulation of the model was developed in [13] for a vibrational system including up to five interacting

bands. The intensity fit of experimental data led to the determination of the dipole moment derivatives  $d_2 = \partial\mu/\partial q_2$  and  $d_5 = \partial\mu/\partial q_5$  relative to the  $\nu_2$  and  $\nu_5$  bands, as well as the first-order Herman-Wallis correction in  $K$  to  $d_5$ . A new evaluation of the individual band strengths  $S_2$  and  $S_5$  is made and compared with previous determinations [7–9].

The following sections present, respectively, the experimental details, the theoretical treatment leading to line intensity data, the procedure used for extracting the individual band strengths  $S_2$  and  $S_5$ , and comparisons with previous works. From the resulting values of the dipole moment derivatives, a global line-by-line prediction is now available for atmospheric applications. For applications of our database to atmospheric remote sensing and retrieval of methyl bromide concentrations, we plan also to investigate line broadening in this region. That work is in progress.

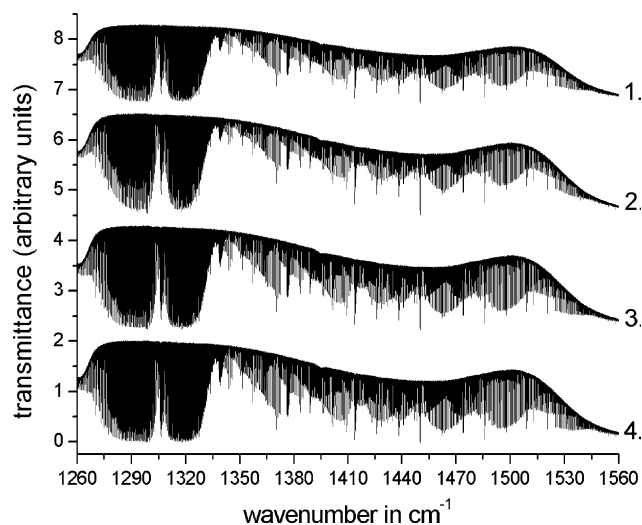


Fig. 1. Unapodized absorption spectra of CH<sub>3</sub>Br between 1260 and 1560 cm<sup>-1</sup>, recorded at a resolution of 0.002 cm<sup>-1</sup> using a Bruker IFS 120 HR located at LADIR (Paris, France), with the experimental conditions reported in Table 1.

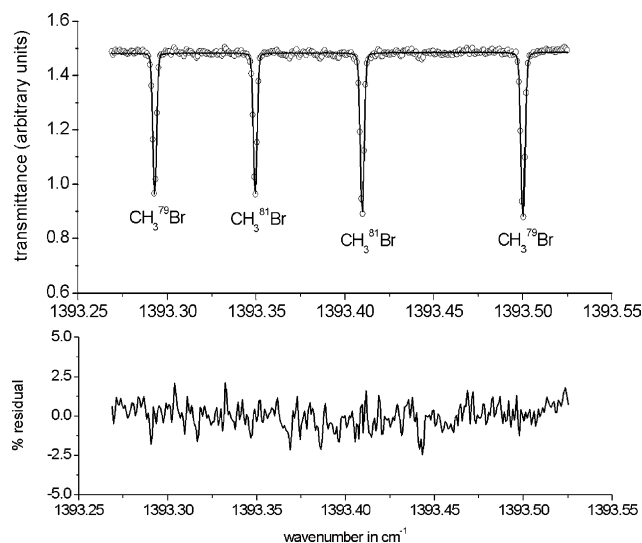


Fig. 2. Line-by-line retrieval of positions and intensities using non-linear least squares fitting technique at 1393 cm<sup>-1</sup>. The differences are minimized by adjusting the assumed positions and intensities of lines in the synthetic spectrum. The methyl bromide gas pressure is 0.4028 ± 0.0016 mbar at 296 ± 1 K, the optical path 415 ± 1 cm, and the resolution is 0.002 cm<sup>-1</sup>. Upper panel: observed (open circles) and synthetic (solid line) spectra overlaid. Lower panel: differences between the two spectra in percent.

## 2. Experimental details

Four absorption spectra of methyl bromide were recorded using a Fourier transform spectrometer Bruker IFS 120 HR. They were not numerically apodized. The instrument was equipped with a MCT photovoltaic detector, a Ge/KBr beamsplitter, and a Globar source. The whole optical path was under vacuum, and a 1.15 mm entrance aperture diameter was used. The MCT detector was used in conjunction with an optical filter, with a bandpass of 1150–1550  $\text{cm}^{-1}$ , to minimize the size of the interferogram data files and also to improve the S/N ratio. In this study, we used a White type multipass cell that provides a  $415 \pm 1$  cm path length. The experimental set-up used in this study was previously described in [14]. All measurements were carried out at room temperature and, during the recording of the spectra, the temperature was continuously monitored using platinum sensors attached inside the cell. The sample of  $\text{CH}_3\text{Br}$ , with bromine at natural abundance (i.e., 50.54%  $^{79}\text{Br}$  and 49.46%  $^{81}\text{Br}$ ), was obtained from Fluka. The chemical purity of  $\text{CH}_3\text{Br}$  was specified to be better than 99%. The sample was used without further purification. To work nearly under Doppler conditions and thus to minimize collisional broadening, the methyl bromide pressures ranged between 0.1991 and 0.4028 mbar and the gas pressure was measured with an absolute uncertainty of 0.4%, using a MKS Baratron gauge with a full-scale reading of 1 mbar. The conditions of absorption path length, pressure, temperature, and resolution are

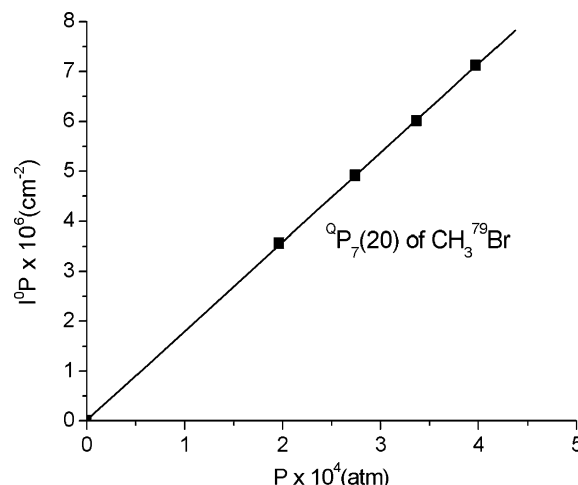


Fig. 3. Pressure dependence: (■) measured values for the  $Q_{P_7(20)}$  line of the  $\nu_2$  band of  $\text{CH}_3^{79}\text{Br}$  with  $I^0 = (1.786 \pm 0.009) \times 10^{-2} \text{ cm}^{-2} \text{ atm}^{-1}$  at 296 K; (—) fits.

provided in Table 1. The experimental uncertainties for temperatures, pressures, and optical paths were estimated to be 1 K, 0.4%, and 1 cm, respectively. Spectral calibration is achieved by using residual water vapour absorptions in the interferometer. Twenty lines of  $\text{H}_2\text{O}$  between 1250–1550  $\text{cm}^{-1}$  were used with reference wavenumbers taken from [15]. The spectral calibration is accurate to  $4.6 \times 10^{-4} \text{ cm}^{-1}$  (RMS). Fig. 1 shows, for the four spectra

Table 2  
Sample of line-by-line measurements of  $\text{CH}_3\text{Br}$  from LADIR FT spectra

	Position ( $\text{cm}^{-1}$ )	Pos – ave <sup>a</sup> ( $\text{cm}^{-1}$ )	Intensity ( $\text{cm}^{-2} \text{ atm}^{-1}$ )	Int – ave <sup>b</sup> (%)	Path (cm)	Pressure (mbar)
	1277.32396	0.00001	0.03182	2.2	415	0.1991
	1277.32394	–0.00001	0.03086	–0.8	415	0.2778
	1277.32394	–0.00001	0.03152	1.3	415	0.3415
	1277.32395	0.00000	0.03029	–2.7	415	0.4028
Average	1277.32395	0.00001	0.03112	1.8		
	1329.02532	0.00001	0.01073	2.0	415	0.1991
	1329.02529	–0.00002	0.01042	–1.1	415	0.2778
	1329.02531	0.00000	0.01072	1.7	415	0.3415
	1329.02530	–0.00001	0.01029	–2.4	415	0.4028
Average	1329.02531	0.00001	0.01054	1.8		
	1406.65865	0.00001	0.01937	–1.0	415	0.1991
	1406.65862	–0.00002	0.01947	–0.5	415	0.2778
	1406.65865	0.00001	0.01993	2.0	415	0.3415
	1406.65865	0.00001	0.01947	–0.5	415	0.4028
Average	1406.65864	0.00001	0.01956	0.8		
	1452.71780	0.00006	0.01037	–1.2	415	0.1991
	1452.71772	–0.00002	0.01049	–0.1	415	0.2778
	1452.71772	–0.00002	0.01067	1.6	415	0.3415
	1452.71772	–0.00002	0.01045	–0.5	415	0.4028
Average	1452.71774	0.00003	0.01050	0.9		
	1525.63592	0.00001	0.02262	5.1	415	0.1991
	1525.63590	–0.00001	0.02109	–2.0	415	0.2778
	1525.63591	0.00000	0.02118	–1.6	415	0.3415
	1525.63590	–0.00001	0.02120	–1.5	415	0.4028
Average	1525.63591	0.00001	0.02152	2.6		

<sup>a</sup> Difference between the individual and averaged position.

<sup>b</sup> Difference between the individual and averaged intensity.

Table 3  
Dipole moment matrix<sup>a</sup> for the Dyad  $\nu_2/\nu_5$  of  $\text{CH}_3^{79}\text{Br}$  and  $\text{CH}_3^{81}\text{Br}$

For $\nu_2$	
$\langle \nu_2 = 0JK \  \mu_Z^T \  \nu_2 = 1JK \rangle = \frac{1}{\sqrt{2}} d_2 K F_{00}(JK)$	
$\langle \nu_2 = 0JK \  \mu_Z^T \  \nu_2 = 1J'K \rangle = \frac{1}{\sqrt{2}} (d_2 + d_2^{(1)} m) F_{10}(mK)$	
For $\nu_5$	
$\langle \nu_5 = 0l_5 = 0JK \  \mu_Z^T \  \nu_5 = 1l_5 = \pm 1JK \pm 1 \rangle = \pm \frac{1}{2} (d_5 \pm d_5^{(2)} (2K \pm 1)) F_{01}^\pm(JK)$	
$\langle \nu_5 = 0l_5 = 0JK \  \mu_Z^T \  \nu_5 = 1l_5 = \pm 1J'K \pm 1 \rangle = \pm \frac{1}{2} (d_5 + d_5^{(1)} m \pm d_5^{(2)} (2K \pm 1)) F_{11}^\pm(mK)$	

Note.  $m = J + 1$  and  $-J$  for  $J' = J + 1$  ( $R$  branch) and  $J - 1$  ( $P$  branch). The expressions of  $F$  functions in terms of  $J$ ,  $m$ , and  $K$  can be found in Table XIV of [19]. The origin of all coefficients can be found in [19].

<sup>a</sup>  $\langle \mu_Z^T \rangle$  is the  $M$ -reduced transition moment defined in [19].

recorded in LADIR, the overviews of the entire  $\nu_2$  and  $\nu_5$  bands of  $\text{CH}_3\text{Br}$ .

Line positions and intensities were retrieved from each individual spectrum using a non-linear least squares fitting technique. Each spectrum was compared to a computed synthetic spectrum and the line positions and intensities were adjusted to reduce the differences between the observed and computed spectra. This treatment was done on intervals smaller than  $0.4 \text{ cm}^{-1}$ , in the range  $1270\text{--}1540 \text{ cm}^{-1}$ . Synthetic spectra were calculated as sums of Voigt profiles and no line mixing was introduced. They were then convoluted with an apparatus function which takes into account the finite path difference and the finite entrance aperture [16]. A sample is shown in Fig. 2. The upper panel shows the observed and synthetic spectra overlaid, and the lower panel shows the difference between the two, in percent. The values of the parameters (positions and intensities) at the end of the adjustment become the “measured” values. An example of the pressure dependence of line intensities is shown on Fig. 3. For each measured line, an average of its position and intensity in the four spectra was carried out, giving the position in  $\text{cm}^{-1}$  and the absolute intensity in  $\text{cm}^{-2} \text{ atm}^{-1}$  at given temperature. In Table 2, a sample of individual measurements and the resulting averages is shown; it is seen that the precisions of the measurements are generally better than 3%. The quantities “Pos – ave” and “Int – ave” are the differences between the individual and averaged values for the positions and intensities, respectively.

### 3. Intensity analysis

#### 3.1. Description of the model

The formulation developed in [13] for  $C_{3v}$  molecules allows to calculate the line positions and intensities for a vibrational system including up to five interacting bands, i.e.,  $2\nu_n, \nu_n + \nu_t, 2\nu_t, \nu_{n'}, \nu_{t'}$ , where  $n$  (or  $n'$ ) and  $t$  (or  $t'$ ) represent non-degenerate  $A$ , or twofold degenerate  $E$  vibrations, respectively. This set of programs has been used in a series of papers related to  $C_{3v}$  symmetric top molecules including  $\text{CH}_3\text{Br}$  [5,6,13,17].

The restriction of this formulation to the dyad system  $\nu_{n'}/\nu_{t'}$  can be quite suitably used in the present intensity analysis of  $\nu_2$  and  $\nu_5$  of  $\text{CH}_3^{79}\text{Br}$  and  $\text{CH}_3^{81}\text{Br}$ . In this

way, the Coriolis coupling between the modes 2 and 5 is calculated via diagonalization. The dipole transition matrix relative to the system  $\nu_2/\nu_5$  is derived from Table 2 of [13] by dropping all the matrix elements except those related to  $\nu_{n'}$  and  $\nu_{t'}$ ; such a matrix is reproduced with specified values of  $n'$  and  $t'$  in Table 3 of the present paper. Nevertheless, in Table 2 of [13], the second order contributions, not required in the present work, are removed so that only five intensity parameters appear in Table 3. The leading intensity parameters are the dipole moment derivatives with respect to the normal coordinate of vibration

$$d_2 = \frac{\partial \mu}{\partial q_2} \quad \text{and} \quad d_5 = \frac{\partial \mu}{\partial q_5}.$$

The first-order contributions depend on three Herman–Wallis type coefficients, i.e.,  $d_2^{(1)}$  and  $d_5^{(1)}$  for the corrections in  $m$  to the leading terms ( $m = -J$  and  $J + 1$  for  $P$  and  $R$  branches, respectively);  $d_5^{(2)}$  for the corrections in  $K$  to the leading term in the degenerate band  $\nu_5$ .

#### 3.2. Intensity analysis and results

The individual-line intensity  $I_{A'}^{B'}$  (in  $\text{cm}^{-2} \text{ atm}^{-1}$  at a temperature  $T$ ) for a transition between two vibrational–rotational states  $A' \rightarrow B'$  is given [18] by

Table 4  
Dipole moment derivatives (in Debye) for the  $\nu_2$  and  $\nu_5$  bands of  $\text{CH}_3^{79}\text{Br}$  and  $\text{CH}_3^{81}\text{Br}$  and Statistical Analysis of the Results<sup>a</sup>

	$\text{CH}_3^{79}\text{Br}$	$\text{CH}_3^{81}\text{Br}$
<i>Dipole moment derivatives</i>		
$d_2$	0.06705(16)	0.06644(18)
$d_5$	0.037819(72)	0.037500(79)
$d_5^{(2)} \times 10^3$	−0.1007(92)	−0.111(10)
<i>Statistics</i>		
$0 \leq \delta I/I < 4\%$	80%	72% of the lines
$4\% \leq \delta I/I < 7\%$	16%	22%
$7\% \leq \delta I/I < 10\%$	2%	3%
$10\% \leq \delta I/I < 17\%$	2%	3%
# lines $\nu_2^c$	59	58
# lines $\nu_5^c$	93	103
% rms $\nu_2$	3.0%	3.3%
% rms $\nu_5$	2.6%	3.0%

<sup>a</sup> The quoted errors are one standard deviation.

<sup>b</sup>  $\delta I/I = (I_{\text{calc}} - I_{\text{obs}})/I_{\text{obs}} \times 100$  in %.

<sup>c</sup> Number of transitions included in the least squares fits.

Table 5  
Comparison between measured and calculated intensities for CH<sub>3</sub><sup>79</sup>Br<sup>a</sup>

	(I)	(II)		(III)	(IV)	(V)	(VI)	(VII)	
(Q)P	(49, A+, 0)	48	A+	0 0	nu2	1269.89052	0.6950E-02	0.7009E-02	0.85
(Q)P	(49, E, 1)	48	E	1 0	nu2	1269.90063	0.6960E-02	0.6849E-02	-1.60
(Q)P	(49, E, 2)	48	E	2 0	nu2	1269.92968	0.6200E-02	0.6390E-02	3.06
(Q)P	(49, A, 3)	48	A	3 0	nu2	1269.97385	0.1150E-01	0.1139E-01	-0.99
(Q)P	(44, A, 6)	43	A	6 0	nu2	1274.30149	0.1130E-01	0.1127E-01	-0.26
(Q)P	(40, A, 3)	39	A	3 0	nu2	1277.32395	0.3110E-01	0.3204E-01	3.01
(Q)P	(39, A+, 0)	38	A+	0 0	nu2	1277.99408	0.2190E-01	0.2178E-01	-0.55
(Q)P	(39, E, 1)	38	E	1 0	nu2	1278.00888	0.2080E-01	0.2127E-01	2.28
(Q)P	(39, E, 2)	38	E	2 0	nu2	1278.05255	0.1930E-01	0.1983E-01	2.75
(Q)P	(39, A, 3)	38	A	3 0	nu2	1278.12241	0.3440E-01	0.3529E-01	2.58
(Q)P	(38, A+, 0)	37	A+	0 0	nu2	1278.78467	0.2390E-01	0.2391E-01	0.03
(Q)P	(38, E, 1)	37	E	1 0	nu2	1278.79993	0.2390E-01	0.2335E-01	-2.29
(Q)P	(38, E, 2)	37	E	2 0	nu2	1278.84493	0.2110E-01	0.2176E-01	3.15
(Q)P	(37, A+, 0)	36	A+	0 0	nu2	1279.57157	0.2600E-01	0.2614E-01	0.55
(Q)P	(37, E, 1)	36	E	1 0	nu2	1279.58726	0.2500E-01	0.2554E-01	2.14
(Q)P	(36, A+, 0)	35	A+	0 0	nu2	1280.35478	0.2780E-01	0.2848E-01	2.45
(Q)P	(36, E, 1)	35	E	1 0	nu2	1280.37090	0.2710E-01	0.2782E-01	2.64
(Q)P	(36, E, 2)	35	E	2 0	nu2	1280.41853	0.2530E-01	0.2592E-01	2.44
(Q)P	(35, A, 3)	34	A	3 0	nu2	1281.27882	0.4790E-01	0.4999E-01	4.35
(Q)P	(35, A, 6)	34	A	6 0	nu2	1281.63790	0.2590E-01	0.2661E-01	2.72
(Q)P	(35, A, 9)	34	A	9 0	nu2	1281.66851	0.9020E-02	0.9568E-02	6.08
(Q)P	(34, A, 3)	33	A	3 0	nu2	1282.05844	0.5150E-01	0.5400E-01	4.86
(Q)P	(32, A, 6)	31	A	6 0	nu2	1284.01067	0.3250E-01	0.3297E-01	1.45
(Q)P	(31, A, 6)	30	A	6 0	nu2	1284.79326	0.3530E-01	0.3511E-01	-0.53
(Q)P	(29, E, 5)	28	E	5 0	nu2	1286.17467	0.2570E-01	0.2550E-01	-0.79
(Q)P	(22, E, 4)	21	E	4 0	nu2	1291.24997	0.3940E-01	0.4096E-01	3.95
(Q)P	(20, E, 7)	19	E	7 0	nu2	1293.36180	0.1790E-01	0.1828E-01	2.14
(Q)P	(10, E, 4)	9	E	4 0	nu2	1299.72939	0.2880E-01	0.2908E-01	0.96
(Q)P	(10, E, 5)	9	E	5 0	nu2	1299.93936	0.2120E-01	0.2111E-01	-0.42
(Q)P	(9, A+, 0)	8	A+	0 0	nu2	1300.03193	0.4510E-01	0.4641E-01	2.90
(Q)P	(9, E, 1)	8	E	1 0	nu2	1300.05542	0.4340E-01	0.4478E-01	3.19
(Q)P	(9, E, 2)	8	E	2 0	nu2	1300.12590	0.3930E-01	0.4021E-01	2.31
(Q)P	(10, A, 6)	9	A	6 0	nu2	1300.19596	0.2880E-01	0.2803E-01	-2.67
(Q)P	(9, A, 3)	8	A	3 0	nu2	1300.24332	0.6370E-01	0.6698E-01	5.15
(Q)P	(9, E, 5)	8	E	5 0	nu2	1300.61919	0.1940E-01	0.1802E-01	-7.12
(Q)P	(8, A+, 0)	7	A+	0 0	nu2	1300.70402	0.4050E-01	0.4233E-01	4.51
(Q)P	(8, E, 1)	7	E	1 0	nu2	1300.72761	0.3890E-01	0.4071E-01	4.65
(Q)R	(3, A+, 0)	4	A+	0 0	nu2	1308.43980	0.2100E-01	0.2259E-01	7.59
(Q)R	(3, E, 1)	4	E	1 0	nu2	1308.46350	0.2050E-01	0.2069E-01	0.93
(Q)R	(4, A+, 0)	5	A+	0 0	nu2	1309.05671	0.2690E-01	0.2783E-01	3.44
(Q)R	(4, E, 1)	5	E	1 0	nu2	1309.08038	0.2510E-01	0.2609E-01	3.96
(Q)R	(20, E, 5)	21	E	5 0	nu2	1318.84184	0.3180E-01	0.3125E-01	-1.74
(Q)R	(25, A, 3)	26	A	3 0	nu2	1321.18440	0.8170E-01	0.8196E-01	0.32
(Q)R	(28, E, 7)	29	E	7 0	nu2	1323.30301	0.1290E-01	0.1260E-01	-2.30
(Q)R	(30, A, 3)	31	A	3 0	nu2	1323.73295	0.6203E-01	0.6263E-01	3.86
(Q)R	(29, E, 7)	30	E	7 0	nu2	1323.78352	0.1170E-01	0.1191E-01	1.76
(Q)R	(33, E, 4)	34	E	4 0	nu2	1325.31036	0.2160E-01	0.2121E-01	-1.80
(Q)R	(40, E, 2)	41	E	2 0	nu2	1328.44252	0.1570E-01	0.1524E-01	-2.93
(Q)R	(40, A, 3)	41	A	3 0	nu2	1328.50147	0.2750E-01	0.2688E-01	-2.25
(Q)R	(41, E, 4)	42	E	4 0	nu2	1329.02531	0.1050E-01	0.1013E-01	-3.49
(Q)R	(41, E, 5)	42	E	5 0	nu2	1329.10019	0.9540E-02	0.8059E-02	-15.52
(Q)R	(44, E, 5)	45	E	5 0	nu2	1330.40355	0.5830E-02	0.5742E-02	-1.50
(Q)R	(44, E, 7)	45	E	7 0	nu2	1330.41647	0.2960E-02	0.3069E-02	3.68
(Q)R	(44, A, 6)	45	A	6 0	nu2	1330.43920	0.8780E-02	0.8646E-02	-1.52
(Q)R	(45, E, 7)	46	E	7 0	nu2	1330.82172	0.2760E-02	0.2720E-02	-1.47
(Q)R	(45, E, 5)	46	E	5 0	nu2	1330.82921	0.5880E-02	0.5092E-02	-13.40
(Q)R	(47, E, 4)	48	E	4 0	nu2	1331.62835	0.5200E-02	0.4985E-02	-4.14
(Q)R	(47, E, 5)	48	E	5 0	nu2	1331.66762	0.4090E-02	0.3961E-02	-3.14
(Q)R	(52, E, 2)	53	E	2 0	nu2	1333.62962	0.3540E-02	0.3396E-02	-4.08
(P)P	(34, A, 6)	33	A	5-1	nu5	1355.71958	0.3390E-02	0.3557E-02	4.92
(P)P	(33, A, 6)	32	A	5-1	nu5	1356.28729	0.3930E-02	0.3958E-02	0.71
(P)P	(27, A, 6)	26	A	5-1	nu5	1359.73452	0.6950E-02	0.6957E-02	0.10
(P)P	(26, A, 6)	25	A	5-1	nu5	1360.31605	0.7230E-02	0.7544E-02	4.34

(continued on next page)

Table 5 (continued)

CH <sub>3</sub> Br: isotope 79									
	(I)	(II)		(III)	(IV)	(V)	(VI)	(VII)	
(P)P	(22, A, 6)	21	A	5-1	nu5	1362.66285	0.9860E-02	0.1004E-01	1.84
(P)Q	(24, E, 7)	24	E	6-1	nu5	1364.32035	0.6910E-02	0.6745E-02	-2.39
(P)Q	(27, E, 7)	27	E	6-1	nu5	1364.51345	0.6190E-02	0.6028E-02	-2.62
(P)Q	(28, E, 7)	28	E	6-1	nu5	1364.58205	0.6000E-02	0.5748E-02	-4.21
(P)P	(13, A, 6)	12	A	5-1	nu5	1368.06777	0.1540E-01	0.1530E-01	-0.65
(P)Q	(38, A, 6)	38	A	5-1	nu5	1377.71318	0.7620E-02	0.7438E-02	-2.38
(P)Q	(39, A, 6)	39	A	5-1	nu5	1377.78830	0.6890E-02	0.6771E-02	-1.73
(P)P	(21, E, 4)	20	E	3-1	nu5	1388.15498	0.7580E-02	0.7664E-02	1.11
(P)P	(33, A, 3)	32	A	2-1	nu5	1393.29286	0.6890E-02	0.7377E-02	7.06
(P)R	(26, A, 6)	27	A	5-1	nu5	1394.19085	0.8600E-02	0.8394E-02	-2.39
(P)P	(11, E, 4)	10	E	3-1	nu5	1394.28182	0.1000E-01	0.9946E-02	-0.54
(P)R	(28, A, 6)	29	A	5-1	nu5	1395.57706	0.8210E-02	0.8060E-02	-1.83
(P)P	(29, A, 3)	28	A	2-1	nu5	1395.66957	0.9930E-02	0.1037E-01	4.42
(P)R	(30, A, 6)	31	A	5-1	nu5	1396.96929	0.7800E-02	0.7564E-02	-3.03
(P)P	(16, A, 3)	15	A	2-1	nu5	1403.55170	0.1920E-01	0.1971E-01	2.66
(P)P	(15, A, 3)	14	A	2-1	nu5	1404.16820	0.2010E-01	0.2004E-01	-0.30
(P)P	(35, E, 2)	34	E	1-1	nu5	1404.30171	0.2960E-02	0.3309E-02	11.80
(P)R	(26, E, 5)	27	E	4-1	nu5	1406.62982	0.5590E-02	0.5512E-02	-1.40
(P)P	(31, E, 2)	30	E	1-1	nu5	1406.68844	0.4910E-02	0.4748E-02	-3.31
(P)R	(12, E, 4)	13	E	3-1	nu5	1409.65085	0.4980E-02	0.4761E-02	-4.39
(P)P	(26, E, 2)	25	E	1-1	nu5	1409.69975	0.6710E-02	0.6805E-02	1.41
(P)P	(21, E, 2)	20	E	1-1	nu5	1412.74290	0.8550E-02	0.8744E-02	2.27
(P)R	(17, E, 4)	18	E	3-1	nu5	1412.96324	0.7180E-02	0.6725E-02	-6.34
(P)P	(28, E, 1)	27	E	0 1	nu5	1420.62785	0.5670E-02	0.5963E-02	5.17
(P)R	(10, A, 3)	11	A	2-1	nu5	1420.70209	0.1130E-01	0.1078E-01	-4.58
(P)R	(11, A, 3)	12	A	2-1	nu5	1421.35653	0.1250E-01	0.1207E-01	-3.46
(P)R	(30, E, 4)	31	E	3-1	nu5	1421.72658	0.6450E-02	0.6086E-02	-5.64
(P)P	(22, E, 1)	21	E	0 1	nu5	1424.29039	0.8160E-02	0.8241E-02	0.99
(P)P	(21, E, 1)	20	E	0 1	nu5	1424.90470	0.8380E-02	0.8549E-02	2.02
(P)R	(40, E, 4)	41	E	3-1	nu5	1428.59060	0.3220E-02	0.3105E-02	-3.58
(P)P	(15, E, 1)	14	E	0 1	nu5	1428.61469	0.9320E-02	0.9459E-02	1.49
(P)P	(14, E, 1)	13	E	0 1	nu5	1429.23708	0.9780E-02	0.9403E-02	-3.86
(P)R	(41, E, 4)	42	E	3-1	nu5	1429.28169	0.2860E-02	0.2836E-02	-0.83
(P)R	(23, A, 3)	24	A	2-1	nu5	1429.30402	0.1860E-01	0.1816E-01	-2.37
(P)P	(12, E, 1)	11	E	0 1	nu5	1430.48519	0.8800E-02	0.9073E-02	3.11
(P)R	(26, A, 3)	27	A	2-1	nu5	1431.31581	0.1770E-01	0.1706E-01	-3.59
(P)R	(8, E, 2)	9	E	1-1	nu5	1431.67712	0.6130E-02	0.5838E-02	-4.76
(P)P	(10, E, 1)	9	E	0 1	nu5	1431.73798	0.8210E-02	0.8438E-02	2.78
(R)P	(27, A+, 0)	26	A+	1 1	nu5	1433.67203	0.1220E-01	0.1260E-01	3.32
(P)P	(21, A+, 0)	20	A+	1 1	nu5	1437.20368	0.1590E-01	0.1627E-01	2.36
(P)R	(7, E, 1)	8	E	0 1	nu5	1443.21574	0.7450E-02	0.7003E-02	-6.00
(R)P	(11, A+, 0)	10	A+	1 1	nu5	1443.25944	0.1440E-01	0.1502E-01	4.29
(R)P	(28, E, 1)	27	E	2 1	nu5	1444.64432	0.5260E-02	0.5628E-02	6.99
(P)R	(28, E, 2)	29	E	1-1	nu5	1444.87932	0.9530E-02	0.9222E-02	-3.24
(R)P	(15, E, 1)	14	E	2 1	nu5	1452.68116	0.7090E-02	0.7302E-02	2.99
(R)R	(3, A+, 0)	4	A+	1 1	nu5	1452.73959	0.1070E-01	0.1044E-01	-2.46
(R)R	(12, A+, 0)	13	A+	1 1	nu5	1458.64851	0.2520E-01	0.2533E-01	0.50
(R)R	(15, A+, 0)	16	A+	1 1	nu5	1460.65316	0.2750E-01	0.2770E-01	0.73
(R)R	(16, A+, 0)	17	A+	1 1	nu5	1461.32513	0.2780E-01	0.2815E-01	1.24
(R)R	(8, E, 1)	9	E	2 1	nu5	1467.94322	0.1160E-01	0.1173E-01	1.09
(R)R	(9, E, 1)	10	E	2 1	nu5	1468.58988	0.1210E-01	0.1243E-01	2.72
(R)R	(12, E, 1)	13	E	2 1	nu5	1470.53443	0.1430E-01	0.1412E-01	-1.29
(R)R	(40, A+, 0)	41	A+	1 1	nu5	1477.96040	0.9770E-02	0.9499E-02	-2.77
(R)R	(24, E, 1)	25	E	2 1	nu5	1478.37941	0.1390E-01	0.1382E-01	-0.59
(R)R	(25, E, 1)	26	E	2 1	nu5	1479.03768	0.1390E-01	0.1337E-01	-3.81
(R)R	(7, E, 2)	8	E	3 1	nu5	1479.18452	0.1260E-01	0.1229E-01	-2.43
(R)P	(22, E, 4)	21	E	5 1	nu5	1483.61714	0.3610E-02	0.3643E-02	0.93
(R)R	(33, E, 1)	34	E	2 1	nu5	1484.32695	0.9230E-02	0.8876E-02	-3.84
(R)R	(15, E, 2)	16	E	3 1	nu5	1484.36231	0.1530E-01	0.1535E-01	0.30
(R)R	(20, E, 2)	21	E	3 1	nu5	1487.61895	0.1480E-01	0.1488E-01	0.52
(R)R	(38, E, 1)	39	E	2 1	nu5	1487.65218	0.6290E-02	0.6064E-02	-3.59
(R)R	(21, E, 2)	22	E	3 1	nu5	1488.27203	0.1480E-01	0.1458E-01	-1.47
(R)R	(3, A, 3)	4	A	4 1	nu5	1488.39515	0.2280E-01	0.2279E-01	-0.04
(R)R	(26, E, 2)	27	E	3 1	nu5	1491.54565	0.1250E-01	0.1238E-01	-0.98

(continued on next page)

Table 5 (continued)

CH <sub>3</sub> Br: isotope 79									
	(I)	(II)		(III)	(IV)	(V)	(VI)	(VII)	
(R)R	(8, A, 3)	9	A	4 1	nu5	1491.60898	0.2720E-01	0.2672E-01	-1.77
(R)R	(8, E, 4)	9	E	5 1	nu5	1503.27884	0.1350E-01	0.1305E-01	-3.34
(R)R	(13, E, 4)	14	E	5 1	nu5	1506.50186	0.1360E-01	0.1378E-01	1.33
(R)R	(21, E, 4)	22	E	5 1	nu5	1511.68182	0.1240E-01	0.1235E-01	-0.41
(R)R	(39, A, 3)	40	A	4 1	nu5	1511.81372	0.9700E-02	0.9193E-02	-5.22
(R)R	(23, E, 4)	24	E	5 1	nu5	1512.98061	0.1220E-01	0.1155E-01	-5.31
(R)R	(25, E, 4)	26	E	5 1	nu5	1514.28084	0.1050E-01	0.1064E-01	1.35
(R)R	(43, A, 3)	44	A	4 1	nu5	1514.44453	0.6330E-02	0.6142E-02	-2.97
(R)R	(30, E, 4)	31	E	5 1	nu5	1517.53672	0.8170E-02	0.8118E-02	-0.64
(R)R	(13, E, 5)	14	E	6 1	nu5	1518.05359	0.1250E-01	0.1222E-01	-2.27
(R)R	(31, E, 4)	32	E	5 1	nu5	1518.18872	0.7420E-02	0.7605E-02	2.50
(R)R	(14, E, 5)	15	E	6 1	nu5	1518.69824	0.1250E-01	0.1215E-01	-2.80
(R)R	(32, E, 4)	33	E	5 1	nu5	1518.84096	0.6790E-02	0.7100E-02	4.56
(R)R	(15, E, 5)	16	E	6 1	nu5	1519.34328	0.1220E-01	0.1204E-01	-1.29
(R)R	(33, E, 4)	34	E	5 1	nu5	1519.49334	0.6610E-02	0.6604E-02	-0.10
(R)R	(7, A, 6)	8	A	7 1	nu5	1525.63591	0.2150E-01	0.2104E-01	-2.15
(R)R	(8, A, 6)	9	A	7 1	nu5	1526.27738	0.2110E-01	0.2099E-01	-0.53
(R)R	(9, A, 6)	10	A	7 1	nu5	1526.91919	0.2100E-01	0.2096E-01	-0.21
(R)R	(27, E, 5)	28	E	6 1	nu5	1527.10769	0.8010E-02	0.8145E-02	1.69
(R)R	(11, A, 6)	12	A	7 1	nu5	1528.20380	0.2070E-01	0.2085E-01	0.70
(R)R	(12, A, 6)	13	A	7 1	nu5	1528.84658	0.2090E-01	0.2073E-01	-0.79
(R)R	(14, A, 6)	15	A	7 1	nu5	1530.13299	0.2000E-01	0.2036E-01	1.79
(R)R	(19, A, 6)	20	A	7 1	nu5	1533.35341	0.1920E-01	0.1841E-01	-4.10
(R)R	(22, A, 6)	23	A	7 1	nu5	1535.28825	0.1620E-01	0.1664E-01	2.71
(R)R	(29, A, 6)	30	A	7 1	nu5	1539.80610	0.1130E-01	0.1160E-01	2.68

(I) Lower state quantum numbers. (II) Upper state quantum numbers. (III) Vibrational band. (IV) Observed positions (in cm<sup>-1</sup>). (V) Observed intensities in cm<sup>-2</sup> atm<sup>-1</sup> at 296 K. (VI) Calculated intensities in cm<sup>-2</sup> atm<sup>-1</sup> at 296 K. (VII)  $\frac{I_{\text{calc}}-I_{\text{obs}}}{I_{\text{obs}}} \times 100$  in %.

<sup>a</sup> Symmetry labeling used are A+, A- (A when both the components are unresolved), E following the notation of [13].

$$I_{A''}^{B'} = \frac{8\pi^3}{3hc} \cdot \frac{LT_0}{TQ_T} g_{A''} \cdot \nu_{B' \leftarrow A''} \cdot \left[ 1 - \exp\left(-\frac{hc\nu_{B' \leftarrow A''}}{kT}\right) \right] \cdot \exp\left(-\frac{hcE_{A''}}{kT}\right) \cdot |\langle B' || \mu_Z^t || A'' \rangle|^2. \quad (1)$$

In Eq. (1),  $L = 2.68675 \times 10^{19}$  molecules cm<sup>-3</sup> is the Loschmidt number at  $T_0 = 273.15$  K and  $P = 1$  atm;  $T = 296$  K;  $Q_T = 20762.196$  for CH<sub>3</sub><sup>79</sup>Br and 20849.271 for CH<sub>3</sub><sup>81</sup>Br are the total partition functions at 296 K calculated by Brunetaud et al. [5];  $\nu_{B' \leftarrow A''}$  is the wavenumber of the transition (in cm<sup>-1</sup>);  $g_{A''}$  and  $E_{A''}$  are the total degeneracy and the energy of the lower state, respectively;  $\langle B' || \mu_Z^t || A'' \rangle$  is the  $M$ -reduced transition dipole moment defined in [19],  $|A''\rangle$  and  $|B'\rangle$  are the eigenvectors that can be described as linear combination of the zero-order basis wavefunctions  $|v, l, J, K\rangle$  for the lower and the upper state, respectively,  $c$  is the speed of light, and  $h$  and  $k$  represent the Planck and Boltzmann constants, respectively.

In the present work, no fit of the line positions was performed. The energy parameters for both ground and upper vibrational states were fixed to the values obtained in [6]. The programs described in [13] were used to reproduce the energy levels, line positions, and eigenvectors required for the line intensity calculation.

The absolute intensities of 117 lines of  $\nu_2$  in the range 1269–1333 cm<sup>-1</sup>, and of 196 lines of  $\nu_5$  in the range of 1364–1527 cm<sup>-1</sup>, were measured. The data cover the subbands <sup>Q</sup>P and <sup>Q</sup>R in  $\nu_2$  (with  $J \leq 52$  and  $K \leq 9$ ) and five

subbands <sup>P</sup>Q, <sup>P</sup>P, <sup>P</sup>R, <sup>R</sup>P, and <sup>R</sup>R in  $\nu_5$  (with  $J \leq 50$  and  $K \leq 7$ ).

A least-square fit of the line intensities belonging to  $\nu_2$  and  $\nu_5$  led to the determination of three intensity parameters, for each isotopomers of CH<sub>3</sub>Br. The values of the intensity parameters obtained in our fit are listed in Table 4, together with the statistical analysis of our results. The intensities were reproduced with an overall standard deviation of 3%, which is comparable to the mean experimental uncertainty equal to 4%. One parameter is needed to fit the  $\nu_2$  band within 3.0% for CH<sub>3</sub><sup>79</sup>Br and 3.3% for CH<sub>3</sub><sup>81</sup>Br (the term  $d_2$ , i.e., the first term of the dipole moment transition derivative expansion in  $\nu_2$ ); two parameters are needed to fit the  $\nu_5$  band within 2.6% for CH<sub>3</sub><sup>79</sup>Br and 3.0% for CH<sub>3</sub><sup>81</sup>Br (the terms  $d_5$  and  $d_5^{(2)}$ , i.e., the leading term of the dipole moment transition derivative expansion in  $\nu_5$  and its  $K$  dependence, respectively), according to the notation of Table 3. Without the first-order Herman–Wallis correction in  $K$  to  $d_5$ , the standard deviations become 4.5% for CH<sub>3</sub><sup>79</sup>Br and 4.8% for CH<sub>3</sub><sup>81</sup>Br in  $\nu_5$ . The  $d_2^{(1)}$  and  $d_5^{(1)}$  terms (the  $J$  dependence of the transition dipole moments of  $\nu_2$  and  $\nu_5$ , respectively) were not determined and did not contribute to decrease the standard deviation, so we set them to zero.

The fit of the intensity data was performed according to the same procedure already used for the intensity analysis of  $\nu_2$  and  $\nu_5$  of <sup>12</sup>CH<sub>3</sub><sup>35</sup>Cl and of  $\nu_2$  and  $\nu_5$  of <sup>12</sup>CH<sub>3</sub>F, respectively by Cappellani et al. [20] and by Lepère et al. [21]. These

Table 6  
Comparison between measured and calculated intensities for CH<sub>3</sub><sup>81</sup>Br<sup>a</sup>

CH <sub>3</sub> Br: isotope 81									
	(I)	(II)		(III)	(IV)	(V)	(VI)	(VII)	
(Q)P	(44, A, 6)	43	A	6 0	nu2	1274.40479	0.1150E-01	0.1115E-01	-3.05
(Q)P	(40, A+, 0)	39	A+	0 0	nu2	1277.28621	0.1910E-01	0.1951E-01	2.16
(Q)P	(40, E, 1)	39	E	1 0	nu2	1277.30067	0.1840E-01	0.1906E-01	3.60
(Q)P	(40, E, 2)	39	E	2 0	nu2	1277.34314	0.1680E-01	0.1777E-01	5.78
(Q)P	(39, A+, 0)	38	A+	0 0	nu2	1278.07716	0.2130E-01	0.2149E-01	0.89
(Q)P	(39, E, 1)	38	E	1 0	nu2	1278.09204	0.2040E-01	0.2099E-01	2.90
(Q)P	(39, E, 2)	38	E	2 0	nu2	1278.13590	0.2050E-01	0.1957E-01	-4.55
(Q)P	(38, A+, 0)	37	A+	0 0	nu2	1278.86445	0.2280E-01	0.2358E-01	3.42
(Q)P	(38, E, 1)	37	E	1 0	nu2	1278.87976	0.2260E-01	0.2303E-01	1.91
(Q)P	(36, A+, 0)	35	A+	0 0	nu2	1280.42804	0.2680E-01	0.2806E-01	4.72
(Q)P	(36, E, 1)	35	E	1 0	nu2	1280.44422	0.2700E-01	0.2741E-01	1.52
(Q)P	(35, E, 2)	34	E	2 0	nu2	1281.26991	0.2740E-01	0.2770E-01	1.08
(Q)P	(34, E, 1)	33	E	1 0	nu2	1281.99378	0.3130E-01	0.3212E-01	2.62
(Q)P	(34, E, 2)	33	E	2 0	nu2	1282.04408	0.2880E-01	0.2992E-01	3.88
(Q)P	(32, A, 6)	31	A	6 0	nu2	1284.07296	0.3240E-01	0.3244E-01	0.12
(Q)P	(31, A, 6)	30	A	6 0	nu2	1284.85223	0.3280E-01	0.3453E-01	5.28
(Q)P	(29, E, 5)	28	E	5 0	nu2	1286.22660	0.2460E-01	0.2506E-01	1.85
(Q)P	(28, E, 4)	27	E	4 0	nu2	1286.83011	0.3370E-01	0.3268E-01	-3.02
(Q)P	(26, A, 9)	25	A	9 0	nu2	1289.16711	0.1560E-01	0.1553E-01	-0.47
(Q)P	(22, E, 4)	21	E	4 0	nu2	1291.28002	0.3850E-01	0.4016E-01	4.32
(Q)P	(21, E, 4)	20	E	4 0	nu2	1292.00716	0.4020E-01	0.4081E-01	1.52
(Q)P	(10, E, 4)	9	E	4 0	nu2	1299.72537	0.2840E-01	0.2845E-01	0.17
(Q)P	(10, E, 5)	9	E	5 0	nu2	1299.93533	0.2080E-01	0.2066E-01	-0.69
(Q)P	(9, A+, 0)	8	A+	0 0	nu2	1300.02527	0.4250E-01	0.4540E-01	6.83
(Q)P	(9, E, 1)	8	E	1 0	nu2	1300.04877	0.4100E-01	0.4381E-01	6.86
(Q)P	(9, E, 2)	8	E	2 0	nu2	1300.11921	0.3770E-01	0.3934E-01	4.35
(Q)P	(10, A, 6)	9	A	6 0	nu2	1300.19191	0.2800E-01	0.2742E-01	-2.06
(Q)P	(9, E, 5)	8	E	5 0	nu2	1300.61248	0.1810E-01	0.1763E-01	-2.62
(Q)P	(8, A+, 0)	7	A+	0 0	nu2	1300.69472	0.3900E-01	0.4141E-01	6.17
(Q)P	(8, E, 1)	7	E	1 0	nu2	1300.71832	0.3750E-01	0.3982E-01	6.20
(Q)P	(5, A, 3)	4	A	3 0	nu2	1302.89255	0.3420E-01	0.2849E-01	-16.71
(Q)P	(4, E, 2)	3	E	2 0	nu2	1303.42625	0.1660E-01	0.1520E-01	-8.46
(Q)R	(3, A+, 0)	4	A+	0 0	nu2	1308.40091	0.2100E-01	0.2210E-01	5.23
(Q)R	(3, E, 1)	4	E	1 0	nu2	1308.42468	0.2110E-01	0.2024E-01	-4.09
(Q)R	(4, A+, 0)	5	A+	0 0	nu2	1309.01555	0.2580E-01	0.2722E-01	5.49
(Q)R	(4, E, 1)	5	E	1 0	nu2	1309.03922	0.2510E-01	0.2552E-01	1.68
(Q)R	(4, E, 2)	5	E	2 0	nu2	1309.11020	0.2100E-01	0.2081E-01	-0.90
(Q)R	(21, A+, 0)	22	A+	0 0	nu2	1318.80861	0.5600E-01	0.5791E-01	3.42
(Q)R	(21, E, 1)	22	E	1 0	nu2	1318.82896	0.5270E-01	0.5643E-01	7.07
(Q)R	(25, E, 4)	26	E	4 0	nu2	1321.22845	0.3360E-01	0.3362E-01	0.07
(Q)R	(24, E, 7)	25	E	7 0	nu2	1321.25138	0.1480E-01	0.1479E-01	-0.08
(Q)R	(26, E, 7)	27	E	7 0	nu2	1322.24428	0.1330E-01	0.1367E-01	2.79
(Q)R	(27, E, 4)	28	E	4 0	nu2	1322.25176	0.3080E-01	0.3065E-01	-0.49
(Q)R	(28, E, 7)	29	E	7 0	nu2	1323.21720	0.1200E-01	0.1238E-01	3.20
(Q)R	(29, E, 4)	30	E	4 0	nu2	1323.25720	0.2730E-01	0.2743E-01	0.49
(Q)R	(29, E, 7)	30	E	7 0	nu2	1323.69623	0.1240E-01	0.1170E-01	-5.62
(Q)R	(30, E, 4)	31	E	4 0	nu2	1323.75323	0.2560E-01	0.2579E-01	0.73
(Q)R	(29, A-, 9)	30	A	9 0	nu2	1323.76363	0.9740E-02	0.9684E-02	-0.57
(Q)R	(29, E, 8)	30	E	8 0	nu2	1323.79841	0.8020E-02	0.7836E-02	-2.30
(Q)R	(33, E, 5)	34	E	5 0	nu2	1325.33400	0.1640E-01	0.1661E-01	1.29
(Q)R	(40, E, 4)	41	E	4 0	nu2	1328.47071	0.1140E-01	0.1112E-01	-2.42
(Q)R	(43, A+, 0)	44	A+	0 0	nu2	1329.64147	0.1220E-01	0.1201E-01	-1.52
(Q)R	(43, E, 1)	44	E	1 0	nu2	1329.65284	0.1200E-01	0.1172E-01	-2.36
(Q)R	(45, A, 6)	46	A	6 0	nu2	1330.74695	0.7810E-02	0.7590E-02	-2.82
(Q)R	(50, A+, 0)	51	A+	0 0	nu2	1332.65828	0.5090E-02	0.4960E-02	-2.55
(Q)R	(50, E, 1)	51	E	1 0	nu2	1332.66609	0.5260E-02	0.4837E-02	-8.03
(Q)R	(50, E, 2)	51	E	2 0	nu2	1332.68810	0.4630E-02	0.4486E-02	-3.11
(Q)R	(50, A, 3)	51	A	3 0	nu2	1332.72014	0.8150E-02	0.7908E-02	-2.97
(P)P	(34, A, 6)	33	A	5-1	nu5	1355.77039	0.3400E-02	0.3548E-02	4.35
(P)P	(33, A, 6)	32	A	5-1	nu5	1356.33627	0.3770E-02	0.3946E-02	4.66
(P)P	(27, A, 6)	26	A	5-1	nu5	1359.77221	0.6710E-02	0.6911E-02	3.00
(P)P	(26, A, 6)	25	A	5-1	nu5	1360.35179	0.7080E-02	0.7490E-02	5.80
(P)P	(22, A, 6)	21	A	5-1	nu5	1362.69065	0.9690E-02	0.9951E-02	2.69

(continued on next page)

Table 6 (continued)

CH <sub>3</sub> Br: isotope 81									
	(I)	(II)		(III)	(IV)	(V)	(VI)	(VII)	
(P)Q	(24, E, 7)	24	E	6-1	nu5	1364.29103	0.6620E-02	0.6669E-02	0.74
(P)Q	(25, E, 7)	25	E	6-1	nu5	1364.35274	0.6320E-02	0.6459E-02	2.20
(P)Q	(28, E, 7)	28	E	6-1	nu5	1364.55055	0.5770E-02	0.5690E-02	-1.39
(P)Q	(29, E, 7)	29	E	6-1	nu5	1364.62061	0.5350E-02	0.5402E-02	0.97
(P)P	(17, A, 6)	16	A	5-1	nu5	1365.66135	0.1530E-01	0.1303E-01	-14.86
(P)P	(13, A, 6)	12	A	5-1	nu5	1368.07683	0.1720E-01	0.1511E-01	-12.16
(P)Q	(38, A, 6)	38	A	5-1	nu5	1377.67895	0.7360E-02	0.7387E-02	0.37
(P)Q	(39, A, 6)	39	A	5-1	nu5	1377.75343	0.6410E-02	0.6727E-02	4.95
(P)P	(21, E, 4)	20	E	3-1	nu5	1388.18494	0.7740E-02	0.7569E-02	-2.21
(P)P	(33, A, 3)	32	A	2-1	nu5	1393.34945	0.7010E-02	0.7313E-02	4.32
(P)R	(25, A, 6)	26	A	5-1	nu5	1393.40968	0.8730E-02	0.8368E-02	-4.14
(P)R	(26, A, 6)	27	A	5-1	nu5	1394.09754	0.8530E-02	0.8278E-02	-2.95
(P)P	(11, E, 4)	10	E	3-1	nu5	1394.28993	0.1000E-01	0.9793E-02	-2.07
(P)P	(29, A, 3)	28	A	2-1	nu5	1395.71815	0.1000E-01	0.1026E-01	2.59
(P)P	(27, A, 3)	26	A	2-1	nu5	1396.91084	0.1150E-01	0.1187E-01	3.18
(P)P	(16, A, 3)	15	A	2-1	nu5	1403.57270	0.1860E-01	0.1941E-01	4.34
(P)P	(15, A, 3)	14	A	2-1	nu5	1404.18699	0.1960E-01	0.1973E-01	0.64
(P)R	(23, E, 5)	24	E	4-1	nu5	1404.50316	0.5590E-02	0.5601E-02	0.19
(P)P	(11, A, 3)	10	A	2-1	nu5	1406.65864	0.1960E-01	0.1993E-01	1.71
(P)R	(44, A, 6)	45	A	5-1	nu5	1406.71127	0.3100E-02	0.2806E-02	-9.49
(P)P	(31, E, 2)	30	E	1-1	nu5	1406.74303	0.4650E-02	0.4695E-02	0.96
(P)R	(29, E, 5)	30	E	4-1	nu5	1408.58685	0.5100E-02	0.5000E-02	-1.95
(P)R	(12, E, 4)	13	E	3-1	nu5	1409.60025	0.4850E-02	0.4679E-02	-3.52
(P)P	(26, E, 2)	25	E	1-1	nu5	1409.74401	0.6370E-02	0.6714E-02	5.41
(P)R	(35, E, 5)	36	E	4-1	nu5	1412.71537	0.3720E-02	0.3694E-02	-0.70
(P)P	(21, E, 2)	20	E	1-1	nu5	1412.77650	0.8270E-02	0.8612E-02	4.14
(P)R	(10, A, 3)	11	A	2-1	nu5	1420.65839	0.1070E-01	0.1059E-01	-1.06
(P)P	(28, E, 1)	27	E	0 1	nu5	1420.67807	0.5680E-02	0.5881E-02	3.54
(P)P	(27, E, 1)	26	E	0 1	nu5	1421.28363	0.6480E-02	0.6277E-02	-3.14
(P)R	(11, A, 3)	12	A	2-1	nu5	1421.31025	0.1220E-01	0.1185E-01	-2.88
(P)R	(30, E, 4)	31	E	3-1	nu5	1421.62683	0.6160E-02	0.6003E-02	-2.55
(P)P	(22, E, 1)	21	E	0 1	nu5	1424.32778	0.7760E-02	0.8108E-02	4.49
(P)R	(34, E, 4)	35	E	3-1	nu5	1424.34996	0.5420E-02	0.4840E-02	-10.70
(P)P	(21, E, 1)	20	E	0 1	nu5	1424.93994	0.7980E-02	0.8409E-02	5.38
(P)R	(35, E, 4)	36	E	3-1	nu5	1425.03319	0.4830E-02	0.4535E-02	-6.11
(P)R	(22, A, 3)	23	A	2-1	nu5	1428.55997	0.1790E-01	0.1803E-01	0.72
(R)P	(36, A+, 0)	35	A+	1 1	nu5	1428.57803	0.5850E-02	0.6246E-02	6.76
(P)R	(23, A, 3)	24	A	2-1	nu5	1429.22578	0.1800E-01	0.1786E-01	-0.75
(P)P	(14, E, 1)	13	E	0 1	nu5	1429.25670	0.8950E-02	0.9230E-02	3.13
(P)P	(12, E, 1)	11	E	0 1	nu5	1430.50029	0.8580E-02	0.8903E-02	3.76
(P)R	(43, E, 4)	44	E	3-1	nu5	1430.52869	0.2360E-02	0.2319E-02	-1.74
(P)R	(25, A, 3)	26	A	2-1	nu5	1430.56049	0.1730E-01	0.1724E-01	-0.35
(R)P	(31, A+, 0)	30	A+	1 1	nu5	1431.41349	0.8950E-02	0.9535E-02	6.54
(P)R	(8, E, 2)	9	E	1-1	nu5	1431.64009	0.5760E-02	0.5725E-02	-0.60
(P)P	(10, E, 1)	9	E	0 1	nu5	1431.74848	0.8220E-02	0.8276E-02	0.69
(P)P	(27, A+, 0)	26	A+	1 1	nu5	1433.71858	0.1180E-01	0.1240E-01	5.12
(R)P	(21, A+, 0)	20	A+	1 1	nu5	1437.23853	0.1590E-01	0.1598E-01	0.52
(P)R	(35, A, 3)	36	A	2-1	nu5	1437.29000	0.1090E-01	0.1072E-01	-1.68
(P)R	(7, E, 1)	8	E	0 1	nu5	1443.18273	0.6830E-02	0.6861E-02	0.45
(R)P	(11, A+, 0)	10	A+	1 1	nu5	1443.27310	0.1430E-01	0.1471E-01	2.88
(P)P	(28, E, 1)	27	E	2 1	nu5	1444.69719	0.5440E-02	0.5531E-02	1.67
(P)R	(28, E, 2)	29	E	1-1	nu5	1444.78930	0.9520E-02	0.9077E-02	-4.66
(R)P	(15, E, 1)	14	E	2 1	nu5	1452.70567	0.6960E-02	0.7150E-02	2.73
(R)R	(3, A+, 0)	4	A+	1 1	nu5	1452.71774	0.1050E-01	0.1021E-01	-2.75
(R)R	(12, A+, 0)	13	A+	1 1	nu5	1458.60327	0.2460E-01	0.2479E-01	0.78
(R)R	(15, A+, 0)	16	A+	1 1	nu5	1460.59979	0.2690E-01	0.2713E-01	0.84
(R)R	(16, A+, 0)	17	A+	1 1	nu5	1461.26901	0.2670E-01	0.2757E-01	3.25
(R)R	(8, E, 1)	9	E	2 1	nu5	1467.91017	0.1130E-01	0.1146E-01	1.43
(R)R	(9, E, 1)	10	E	2 1	nu5	1468.55427	0.1210E-01	0.1215E-01	0.41
(R)R	(27, A+, 0)	28	A+	1 1	nu5	1468.74729	0.2320E-01	0.2299E-01	-0.91
(R)R	(12, E, 1)	13	E	2 1	nu5	1470.49118	0.1370E-01	0.1380E-01	0.74
(R)R	(40, A+, 0)	41	A+	1 1	nu5	1477.83330	0.1000E-01	0.9373E-02	-6.27
(R)R	(5, E, 2)	6	E	3 1	nu5	1477.87236	0.1150E-01	0.1073E-01	-6.74
(R)R	(6, E, 2)	7	E	3 1	nu5	1478.51334	0.1190E-01	0.1137E-01	-4.43

(continued on next page)

Table 6 (continued)

CH <sub>3</sub> Br: isotope 81									
	(I)	(II)		(III)	(IV)	(V)	(VI)	(VII)	
(R)R	(25, E, 1)	26	E	2 1	nu5	1478.96023	0.1300E-01	0.1311E-01	0.81
(R)R	(7, E, 2)	8	E	3 1	nu5	1479.15501	0.1210E-01	0.1200E-01	-0.82
(R)R	(48, A+, 0)	49	A+	1 1	nu5	1483.53552	0.4100E-02	0.3935E-02	-4.03
(R)R	(32, E, 1)	33	E	2 1	nu5	1483.56710	0.9470E-02	0.9303E-02	-1.77
(R)R	(15, E, 2)	16	E	3 1	nu5	1484.31241	0.1500E-01	0.1499E-01	-0.05
(R)R	(38, E, 1)	39	E	2 1	nu5	1487.53893	0.6620E-02	0.5970E-02	-9.82
(R)R	(20, E, 2)	21	E	3 1	nu5	1487.55600	0.1440E-01	0.1455E-01	1.03
(R)R	(3, A, 3)	4	A	4 1	nu5	1488.37648	0.2160E-01	0.2222E-01	2.86
(R)R	(44, E, 1)	45	E	2 1	nu5	1491.52973	0.3390E-02	0.3363E-02	-0.79
(R)R	(8, A, 3)	9	A	4 1	nu5	1491.57782	0.2590E-01	0.2605E-01	0.59
(R)R	(26, A, 3)	27	A	4 1	nu5	1503.21442	0.2190E-01	0.2244E-01	2.45
(R)R	(8, E, 4)	9	E	5 1	nu5	1503.24838	0.1280E-01	0.1271E-01	-0.73
(R)R	(13, E, 4)	14	E	5 1	nu5	1506.45869	0.1390E-01	0.1343E-01	-3.40
(R)R	(31, A, 3)	32	A	4 1	nu5	1506.47203	0.1700E-01	0.1702E-01	0.12
(R)R	(39, A, 3)	40	A	4 1	nu5	1511.70032	0.1010E-01	0.9037E-02	-10.52
(R)R	(41, A, 3)	42	A	4 1	nu5	1513.00974	0.7620E-02	0.7445E-02	-2.29
(R)R	(43, A, 3)	44	A	4 1	nu5	1514.31987	0.6360E-02	0.6049E-02	-4.89
(R)R	(48, A, 3)	49	A	4 1	nu5	1517.59750	0.3370E-02	0.3390E-02	0.59
(R)R	(13, E, 5)	14	E	6 1	nu5	1518.01087	0.1220E-01	0.1189E-01	-2.56
(R)R	(31, E, 4)	32	E	5 1	nu5	1518.09806	0.7690E-02	0.7444E-02	-3.20
(R)R	(14, E, 5)	15	E	6 1	nu5	1518.65299	0.1210E-01	0.1182E-01	-2.28
(R)R	(32, E, 4)	33	E	5 1	nu5	1518.74755	0.7140E-02	0.6951E-02	-2.64
(R)R	(15, E, 5)	16	E	6 1	nu5	1519.29543	0.1160E-01	0.1172E-01	1.05
(R)R	(33, E, 4)	34	E	5 1	nu5	1519.39730	0.6780E-02	0.6468E-02	-4.60
(R)R	(22, E, 5)	23	E	6 1	nu5	1523.80159	0.9830E-02	0.9965E-02	1.38
(R)R	(7, A, 6)	8	A	7 1	nu5	1525.60865	0.1990E-01	0.2043E-01	2.66
(R)R	(8, A, 6)	9	A	7 1	nu5	1526.24761	0.2030E-01	0.2038E-01	0.40
(R)R	(9, A, 6)	10	A	7 1	nu5	1526.88691	0.1960E-01	0.2035E-01	3.84
(R)R	(11, A, 6)	12	A	7 1	nu5	1528.16647	0.1980E-01	0.2025E-01	2.28
(R)R	(12, A, 6)	13	A	7 1	nu5	1528.80667	0.2010E-01	0.2015E-01	0.23
(R)R	(14, A, 6)	15	A	7 1	nu5	1530.08798	0.1980E-01	0.1979E-01	-0.07
(R)R	(19, A, 6)	20	A	7 1	nu5	1533.29555	0.1830E-01	0.1791E-01	-2.11
(R)R	(22, A, 6)	23	A	7 1	nu5	1535.22243	0.1640E-01	0.1620E-01	-1.22
(R)R	(29, A, 6)	30	A	7 1	nu5	1539.72182	0.1110E-01	0.1132E-01	1.99

(I) Lower state quantum numbers. (II) Upper state quantum numbers. (III) Vibrational band. (IV) Observed positions (in cm<sup>-1</sup>). (V) Observed intensities in cm<sup>-2</sup> atm<sup>-1</sup> at 296 K. (VI) Calculated intensities in cm<sup>-2</sup> atm<sup>-1</sup> at 296 K. (VII)  $\frac{I_{\text{calc}}-I_{\text{obs}}}{I_{\text{obs}}} \times 100$  in %.

<sup>a</sup> Symmetry labeling used are A+, A- (A when both the components are unresolved), E following the notation of [13].

authors also introduced in their fit the Herman-Wallis coefficient  $d_5^{(2)}$  which induced a small variation in  $K$  for  $d_5$ .

The results of this work confirm a positive sign of the Coriolis intensity perturbation  $d_2 \times \zeta_{2,5} \times d_5$ , as predicted in our previous work [6].  $\zeta_{2,5}$  is the Coriolis coupling term between the two bands  $\nu_2$  and  $\nu_5$ , see [6] for more details.

Tables 5 and 6 show a comparison between measured and calculated intensities for both isotopomers of CH<sub>3</sub>Br. Columns (I) to (VII) of these tables give for each transition the following parameters: (I) assignment including the identification of the lower energy level by  $J''$ , symmetry species  $I''$  and  $|K|''$ ; (II) identification of the upper energy level by  $J'$ ,  $I'$ ,  $|K|'$ , and the vibrational angular momentum quantum number  $l'$ ; (III) vibrational band; (IV) observed wavenumbers in cm<sup>-1</sup>; (V) observed intensities  $I_{\text{obs}}$  (in cm<sup>-2</sup> atm<sup>-1</sup> at 296 K); calculated intensities  $I_{\text{calc}}$  (in cm<sup>-2</sup> atm<sup>-1</sup> at 296 K); and the difference between calculated and observed intensities in percent  $\frac{I_{\text{calc}}-I_{\text{obs}}}{I_{\text{obs}}} \times 100$ .

The present line intensity analysis combined with the assignments and line positions of Kwabia Tchana et al. [6] provides an improved CH<sub>3</sub>Br compilation at 7 μm for

databases such as HITRAN [11] and GEISA [12]. To illustrate the quality of our results, Fig. 4 shows the observed and calculated spectra of methyl bromide from 1420 to 1423 cm<sup>-1</sup>. The observed spectrum was recorded at 0.004 cm<sup>-1</sup> resolution, with an optical path of 27.0 ± 0.1 cm and a pressure of 4.693 ± 0.005 mbar at 296 ± 1 K (see [6] for more details).

The vibrational transition dipole moments  $\langle \mu_{\nu} \rangle$  are directly related to the dipole moment derivatives  $|d_2|$  or  $|d_5|$  and were found to be

$$\begin{aligned} \langle |\mu_2| \rangle_{79} &= |d_2|/\sqrt{2} = 0.04741(11) \text{ D and } \langle |\mu_5| \rangle_{79} = |d_5| \\ &= 0.037819(72) \text{ D for CH}_3^{79}\text{Br} \end{aligned} \quad (2)$$

and

$$\begin{aligned} \langle |\mu_2| \rangle_{81} &= |d_2|/\sqrt{2} = 0.04698(13) \text{ D and } \langle |\mu_5| \rangle_{81} = |d_5| \\ &= 0.037500(79) \text{ D for CH}_3^{81}\text{Br.} \end{aligned} \quad (3)$$

The vibrational band strengths  $S_2$  and  $S_5$  of the  $\nu_2$  and  $\nu_5$  bands were calculated from

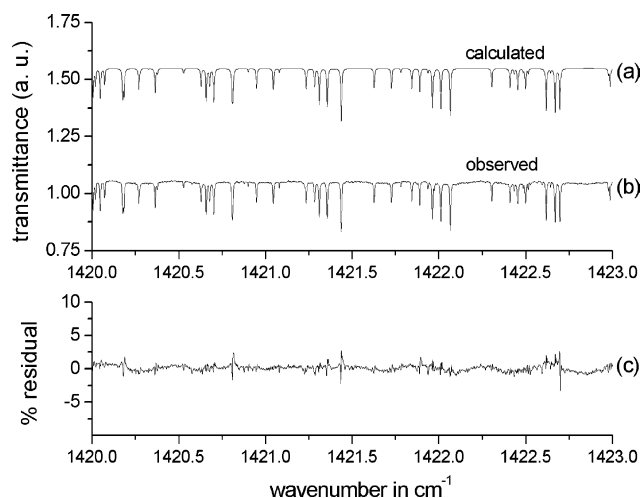


Fig. 4. Comparison between calculated and observed spectra in the 1420–1423  $\text{cm}^{-1}$  interval. Upper panel: (a) synthetic spectrum calculated by using the intensity parameters obtained in this work, (b) observed spectrum recorded at a resolution of  $0.004 \text{ cm}^{-1}$  using a Bruker IFS 120 HR located at LPPM (Orsay, France) [6]. The methyl bromide gas pressure is  $4.693 \pm 0.005 \text{ mbar}$  at  $296 \pm 1 \text{ K}$ , and the optical path  $27.0 \pm 0.1 \text{ cm}$ . Lower panel: (c) differences between observed and calculated spectra (always lower than 5%).

$$S_v = \frac{8\pi^3}{3hc} L \frac{T_0}{T} \left[ \frac{v_v^{79}}{Q_v^{79}} \langle |\mu_v| \rangle_{79}^2 + \frac{v_v^{81}}{Q_v^{81}} \langle |\mu_v| \rangle_{81}^2 \right], \quad (4)$$

where  $Q_v$  is the vibrational partition function ( $Q_v = 1.078522$  and  $1.078806$  for  $\text{CH}_3^{79}\text{Br}$  and  $\text{CH}_3^{81}\text{Br}$ , respectively); and  $v_v^{79}$  and  $v_v^{81}$  are the wavenumbers at the  $\nu_2$  and  $\nu_5$  bands centers of each isotope ( $v_2^{79} = 1305.928849(57) \text{ cm}^{-1}$ ,  $v_2^{81} = 1305.899488(49) \text{ cm}^{-1}$ ,  $v_5^{79} = 1442.931213(44) \text{ cm}^{-1}$ , and  $v_5^{81} = 1442.919224(43) \text{ cm}^{-1}$ ). The values derived for  $S_2$  and  $S_5$  are  $S_2 = 55.7(0.6) \text{ cm}^{-2} \text{ atm}^{-1}$  at  $T = 296 \text{ K}$  and  $S_5 = 39.2(0.3) \text{ cm}^{-2} \text{ atm}^{-1}$  at  $T = 296 \text{ K}$ . To evaluate the consistency of the treatment, a comparison between these values and the values of the sum of all calculated single-line intensities  $\sum I_i$  in  $\text{cm}^{-2} \text{ atm}^{-1}$  (from Eq. (1)), is made for  $\nu_2$  and  $\nu_5$  at  $T = 296 \text{ K}$ . The values obtained for  $\nu_2$  and  $\nu_5$  are  $\sum I_2 = 54.3(2.2) \text{ cm}^{-2} \text{ atm}^{-1}$  at  $T = 296 \text{ K}$  and  $\sum I_5 = 39.5(1.6) \text{ cm}^{-2} \text{ atm}^{-1}$  at  $T = 296 \text{ K}$ . These values are very close to the vibrational band strengths  $S_2$  and  $S_5$  obtained in this work.

#### 4. Discussion

The vibrational band strengths obtained in this study are shown in Table 7 together with those obtained from previous investigations. In the present study, the vibrational band strengths  $S_2$  and  $S_5$  were derived for the first time by an analysis of individual line intensities. The values of [7–9] were determined from integrated band absorptions, using band separation techniques applied on low-resolution spectra. The integrated band intensities obtained from [7–9] are  $A_2 = 67.7$  [7],  $57.4(1.6)$  [8],  $63.4(2.4)$  [9] and  $A_5 = 40.0$  [7],  $49.3(1.3)$  [8],  $51.8(2.4)$  [9], in  $\text{cm}^{-2} \text{ atm}^{-1}$  at  $296 \text{ K}$ . These data probably do

Table 7  
Vibrational band strength of  $\nu_2$  and  $\nu_5$  of  $\text{CH}_3^{79/81}\text{Br}$  (in  $\text{cm}^{-2} \text{ atm}^{-1}$  at  $296 \text{ K}$ )

Ref.	This work <sup>a</sup>	[9]	[8]	[7]
$S_2$	55.7(0.6)	58.8(2.2) <sup>b</sup>	53.2(1.5) <sup>b</sup>	62.7 <sup>b</sup>
$S_5$	39.2(0.3)	48.0(2.2) <sup>b</sup>	45.7(1.2) <sup>b</sup>	37.1 <sup>b</sup>
$S_2 + S_5$	94.9(0.9)	106.8(4.4) <sup>b</sup>	98.9(2.7) <sup>b</sup>	99.8 <sup>b</sup>
$S_2/S_5$	1.42(3)	1.2(1)	1.16(6)	1.7
$(d_2/d_5)^{79}$	1.773(8)			
$(d_2/d_5)^{81}$	1.772(9)			
$\sum I_2$	54.3(2.2) <sup>c</sup>			
$\sum I_5$	39.5(1.6) <sup>c</sup>			

<sup>a</sup> The quoted errors are one standard deviation.

<sup>b</sup> Integrated band intensities  $S_i \equiv A/Q_v$  (see Eq. (5) and text).

<sup>c</sup> Sum of all calculated single-line intensities  $\sum I_i$  in  $\text{cm}^{-2} \text{ atm}^{-1}$  at  $296 \text{ K}$ . The sum of all calculated single-line intensities has been given with an estimated 4% precision (see Table 4).

not represent exactly the band strengths  $S_2$  and  $S_5$  of  $\text{CH}_3\text{Br}$ , because these authors do not discuss any hot band corrections. For example, Fig. 5 shows the contribution of the hot band  $\nu_5 + \nu_3 - \nu_3$ , centered at  $1447.08 \text{ cm}^{-1}$ , to the band strength  $S_5$ .

To compare our result with earlier measurements obtained at low resolution from the integrated band absorption intensity  $A$  including all hot bands in the  $\nu_2$  and  $\nu_5$  regions, we have used the relation

$$S_v \cong A/Q_v, \quad (5)$$

where  $Q_v$  is the vibrational partition function and  $S_v$  the integrated band absorption intensity without hot bands. Employing the values of the integrated band absorption intensity  $A$  from [7–9], and using Eq. (5), we derive the values of  $S_2$ ,  $S_5$ , and  $S_2 + S_5$  (in  $\text{cm}^{-2} \text{ atm}^{-1}$ ) for [7–9], given in Table 7.

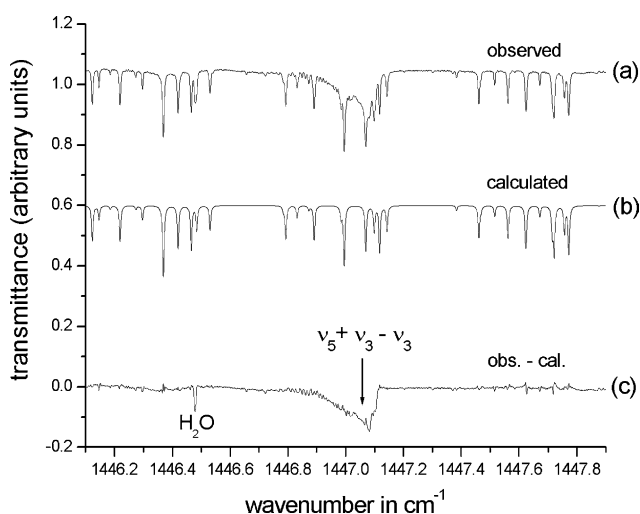


Fig. 5. Comparison between calculated and observed spectra in the  $1446.2\text{--}1447.8 \text{ cm}^{-1}$  interval: (a) observed spectrum recorded at a resolution of  $0.004 \text{ cm}^{-1}$ , with an optical path of  $27.0 \pm 0.1 \text{ cm}$  and a pressure of  $4.693 \pm 0.005 \text{ mbar}$  at  $296 \pm 1 \text{ K}$ ; (b) calculated spectrum; (c) difference between observed and calculated spectra (obs – cal). The presence of the hot band  $\nu_5 + \nu_3 - \nu_3$ , centered at  $1447.08 \text{ cm}^{-1}$  is clearly visible.

Our values are close to the averages of the previous references ( $58.2 \text{ cm}^{-2} \text{ atm}^{-1}$  for  $S_2$  and  $43.6 \text{ cm}^{-2} \text{ atm}^{-1}$  for  $S_5$ ) but the values of  $S_5$  from [8,9] are higher than ours, while the value from the oldest study [7] is lower. Our value of  $S_2$  is in good agreement with the values of [8,9] and moderate agreement is observed with the value of [7].

However, the value of the sum  $S_2 + S_5$  obtained in this work is in very good agreement with the values of [7,8], the percentage difference between our value and the values of [7,8] is less than 6%. The values calculated for the ratio  $S_2/S_5$  are between 1.2 and 1.7.

In the Northwest Infrared (NWIR) database [22], the following values are reported for  $A_2$  and  $A_5$ :  $A_2 = 64.0$  and  $A_5 = 44.0$ , in  $\text{cm}^{-2} \text{ atm}^{-1}$  at 296 K. According to Eq. (5), the following values are derived for  $S_2$  and  $S_5$ :  $S_2 = 59.3 \text{ cm}^{-2} \text{ atm}^{-1}$  and  $S_5 = 40.8 \text{ cm}^{-2} \text{ atm}^{-1}$ . These values are in good agreement with those obtained in this work.

In conclusion, the present analysis makes use of individual line intensities accurately measured and carefully selected and is based on intensity calculations accounting for rovibrational interaction between  $\nu_2$  and  $\nu_5$ . It should improve our knowledge of the intensity parameters of the  $\nu_2$  and  $\nu_5$  fundamentals of  $\text{CH}_3\text{Br}$ .

## 5. Conclusions

The aim of this work was to determine the values of intensity parameters for the fundamental bands  $\nu_2$  and  $\nu_5$ . For that, we measured 313 line intensities, chosen to be well distributed among the two bands  $\nu_2$  and  $\nu_5$ . Modeling of the intensities was achieved within a dyad system. This model is required to account for the rather large Coriolis coupling  $\nu_2/\nu_5$ . The intensities were reproduced with an overall standard deviation of 3.0%, to be compared to a mean experimental uncertainty equal to 4%. For the first time, the band strengths  $S_2$  and  $S_5$  were derived by an analysis of individual line intensities.

A list of lines, in ASCII text format, providing the same information as Tables 5 and 6 with the addition of the energy of the lower level of each transitions, is available on request from one of the authors (E-mail: fkwabia@yahoo.fr).

## Acknowledgments

This work was supported by the Programme National de Chimie Atmosphérique (PNCA). The authors are grateful to

G. Tarrago, who kindly provided her codes for calculation of positions and intensities of  $C_{3v}$  symmetric-top molecules.

## References

- [1] J.H. Butler, Geophys. Res. Lett. 21 (1994) 185.
- [2] R.J. Cicerone, Science 263 (1994) 1243.
- [3] World Meteorological Organization (WMO), "Scientific Assessment of Ozone Depletion: 1998", Report 44, WMO Global Ozone Research and Monitoring Project, Geneva, Switzerland, 1999, Chapter 2.
- [4] G. Graner, J. Mol. Spectrosc. 90 (1981) 394.
- [5] E. Brunetaud, I. Kleiner, N. Lacome, J. Mol. Spectrosc. 216 (2002) 30.
- [6] F. Kwabia Tchana, I. Kleiner, J. Orphal, N. Lacome, O. Bouba, J. Mol. Spectrosc. 228 (2004) 441.
- [7] G.M. Barrow, D.C. McKean, Proc. R. Soc. Lond. Ser. A 213 (1952) 27.
- [8] A.D. Dickson, I.M. Mills, B.L. Crawford Jr., J. Chem. Phys. 27 (1957) 445.
- [9] A.J. Van Straten, W.M.A. Smit, J. Chem. Phys. 67 (1977) 970.
- [10] C. Anastasi, A.E. Heathfield, G.P. Knight, F. Nicolaisen, Spectrochim. Acta Part A 50 (1994) 1791.
- [11] L.S. Rothman, D. Jacquemart, A. Barbe, D. Chris Benner, M. Birk, L.R. Brown, M.R. Carleer, C. Chackerian Jr., K. Chance, L.H. Coudert, V. Dana, V.M. Devi, J.-M. Flaud, R.R. Gamache, A. Goldman, J.-M. Hartmann, K.W. Jucks, A.G. Maki, J.-Y. Mandin, S.T. Massie, J. Orphal, A. Perrin, C.P. Rinsland, M.A.H. Smith, J. Tennyson, R.N. Tolchenov, R.A. Toth, J. Vander Auwera, P. Varanasi, G. Wagner, J. Quant. Spectrosc. Radiat. Transfer 96 (2005) 139.
- [12] N. Jacquinet-Husson, E. Arié, A. Barbe, L.R. Brown, C. Camy-Peyret, J.P. Champion, A. Chedin, A. Chursin, C. Clerbaux, G. Duxbury, J.-M. Flaud, N. Fourrie, A. Fayt, G. Graner, R.R. Gamache, A. Goldman, G. Guelachvili, J.-M. Hartmann, J.C. Hillico, G. Lefevre, V. Naumenko, A. Nikitin, J. Orphal, A. Perrin, D. Reuter, L. Rosenmann, L.S. Rothman, N.A. Scott, J. Selby, L.N. Sinitisa, J.M. Sirota, A. Smith, V.G. Tyuterev, R.H. Tipping, S. Urban, P. Varanasi, M. Weber, J. Quant. Spectrosc. Radiat. Transfer 62 (1999) 205.
- [13] G. Tarrago, J. Mol. Spectrosc. 139 (1990) 439.
- [14] E. Arié, N. Lacome, A. Lévy, Appl. Opt. 26 (1987) 1636.
- [15] R.A. Toth, J. Opt. Soc. Am. B 8 (1991) 2236.
- [16] V. Dana, J.-Y. Mandin, J. Quant. Spectrosc. Radiat. Transfer 48 (1992) 725.
- [17] L.R. Brown, R.L. Sams, I. Kleiner, C. Cottaz, L. Sagui, J. Mol. Spectrosc. 215 (2002) 178.
- [18] M.A.H. Smith, C.P. Rinsland, B. Fridovich, K.N. Rao, in: K. Narahari Rao (Ed.), Molecular Spectroscopy: Modern Research, 3, Academic Press, San Diego, 1985, pp. 111–248.
- [19] G. Tarrago, O.N. Ulenikov, G. Poussigues, J. Phys. 45 (1984) 1429.
- [20] F. Cappellani, G. Restelli, G. Tarrago, J. Mol. Spectrosc. 146 (1991) 326.
- [21] M. Lepère, G. Blanquet, J. Walrand, G. Tarrago, J. Mol. Spectrosc. 189 (1998) 137.
- [22] S.W. Sharpe, T.J. Johnson, R.L. Sams, P.M. Chu, G.C. Rhoderick, P.A. Johnson, Appl. Spectrosc. 58 (12) (2004) 1452.